

Effects of the electron-beam absorption dose on the glass transition, thermal expansion, dynamic mechanical properties, and water uptake of polycardanol containing epoxy groups cured by an electron beam

Jinsil Cheon, Donghwan Cho

Department of Polymer Science and Engineering, Kumoh National Institute of Technology, Gumi, Gyeongbuk 730-701, Korea
Correspondence to: D. Cho (E-mail: dcho@kumoh.ac.kr)

ABSTRACT: In this study, the glass transition, thermal expansion, dynamic mechanical properties, and water-uptake behaviors of diepoxidized polycardanol (DEPC) cured by electron-beam radiation in the presence of cationic photoinitiators were investigated. How the type and concentration of cationic photoinitiators and the electron-beam absorption dose influenced the properties of the cured DEPC was also studied. Two types of cationic photoinitiators, triarylsulfonium hexafluorophosphate (simply referred to as phosphate type or P-type) and triarylsulfonium hexafluoroantimonate (simply referred to as antimonate type or Sb-type), were used. Electron-beam absorption doses of 200, 300, 400, and 600 kGy were applied to the uncured diepoxidized cardanol (DEC) samples, respectively. It was revealed that the Sb-type photoinitiator was preferable to the electron-beam curing of DEC; this led to a lower photoinitiator concentration and/or a lower electron-beam absorption dose compared to that in the phosphate-type photoinitiator. As a result, the variations in the glass-transition temperature, coefficient of thermal expansion, storage modulus, and water uptake of the cured DEPC were quite consistent with each other. We found that the optimal conditions for the enhanced properties of DEPC by electron-beam curing were an Sb-type photoinitiator at 2 wt % and an electron-beam absorption dose of 600 kGy. © 2015 Wiley Periodicals, Inc. *J. Appl. Polym. Sci.* **2015**, *132*, 42570.

KEYWORDS: biopolymers and renewable polymers; crosslinking; glass transition; irradiation; thermal properties

Received 25 November 2014; accepted 1 June 2015

DOI: 10.1002/app.42570

INTRODUCTION

Recently, many research efforts have been devoted to the replacement of petroleum-derived organic materials with environmentally friendly polymer materials because of increasing environmental awareness, social consciousness, and potential industrial impact. A number of such materials have been derived from naturally renewable resources, in particular from plants.^{1–4}

Cardanol, which can be obtained by the thermal treatment of cashew nut shell liquid (CNSL), is a phenol derivative mainly composed of the meta substitute of a C15 unsaturated hydrocarbon chain with one to three double bonds.^{2,5} CNSL is a naturally abundant, low-cost, and renewable material. Polycardanol is viscous and thermally curable, and it has no volatile organic compounds. Therefore, it has some potential as a thermosetting resin for an environmentally friendly biocomposite matrix and also as glossy formaldehyde-free coatings, finishes, and adhesives.^{3,6–8} Diepoxidized cardanol (DEC) is a CNSL-based cardanol derivative; it can be synthesized by enzymatic polymerization routes, and it is also thermally curable to give transpar-

ent films with a high gloss surface and good hardness.² The chemical structure of the DEC is similar to that of cardanol. It seems that the unsaturated double bonds in the chain of cardanol molecules are substituted with two epoxide groups in the DEC molecule. One epoxide group is in the chain end, and the other one is in the middle of the alkyl chain of the molecule, as shown in Figure 1. It has been reported that an epoxide-containing cardanol-based thin film can also be cured by the manner used for epoxy curing. That is, it can be cured by ultraviolet irradiation⁹ and thermal treatment.²

Thermally cured epoxy and epoxy-derived products exhibit, in general, a high extent of curing and good mechanical and thermal properties. However, the thermal curing process of epoxy resins needs a longer processing time and a high processing cost and curing temperature in many applications and a relatively large amount of curing agents.¹⁰ Electron-beam curing can be performed with high-energy electrons from an accelerator to initiate the polymerization and crosslinking of a resin.¹¹ There are many advantages of electron-beam curing over conventional thermal curing of epoxy or epoxy-related resins: short curing time, ambient curing temperature, environmentally friendly, a

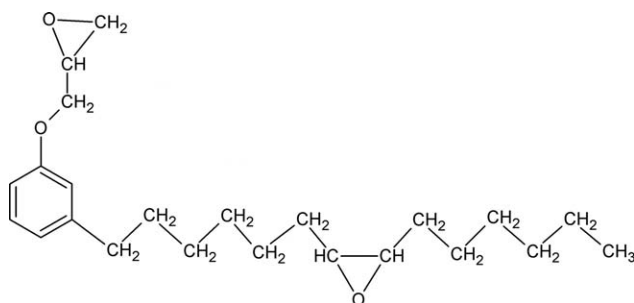


Figure 1. Chemical structure of DEC.

dry and fast process, unlimited materials shelf life, material design flexibility, irradiation uniformity, and labor safety.^{12–15} Also, unlike the thermal curing of epoxy, normally with a relatively large amount of organic curing agent (e.g., amines), a small amount of photoinitiator is used in an epoxy curing process by an electron beam. Accordingly, epoxy curing by electron-beam technology has been studied by a number of research scientists and engineers for many years.^{11,16–18}

It is known that the curing of epoxy resins by electron beams can be successfully processed in the presence of cationic initiators.^{19–22} The cationic radicals generated by electron-beam radiation of the epoxy molecules may react with activated hydrogen molecules in the epoxy groups. Through a series of chemical reaction routes, three-dimensional network structure can finally be formed in the cured epoxy. The mechanism of electron-beam curing of epoxy resin is described in elsewhere.^{10,13} Crivello *et al.*^{17,18} reported the electron-beam-induced cationic polymerization of epoxy in the presence of onium salt photoinitiators. Nishitsuji *et al.*¹⁰ reported a study of the electron-beam-curing process of an epoxy system with the addition of a cationic initiator to investigate the optimal radiation process parameters. Most recently, we reported thermogravimetric and Fourier transform infrared spectroscopic results of the curing behavior of polycardanol containing epoxy groups cured by electron-beam technology.²³

Consequently, the objective of this study was, for the first time, to explore the thermal properties and water absorption resistance of diepoxydized polycardanol (DEPC) cured by electron-beam technology in the presence of cationic photoinitiators in terms of the glass-transition temperature (T_g), thermal expansion, dynamic mechanical properties, and water-uptake behavior. We also discuss how the type and concentration of cationic photoinitiators and the electron-beam absorption dose influenced their properties. The ultimate aim of the study was to provide optimal conditions for the electron-beam curing of DEPC on the basis of our findings.

EXPERIMENTAL

Materials

The DEC resin used for electron-beam curing to prepare the DEPC in this study, which was synthesized via enzymatic polymerization from CNSL, was supplied from the Korea Research Institute of Chemical Technology (Daejeon, Korea). The chemical structure is shown in Figure 1. The color of the thermally curable DEC in the liquid state is light brown before curing.

The molecular weight of DEC was 450 mol/g, and the viscosity was 130–150 cp.

Two different types of photoinitiator onium salts were used for the electron-beam curing of DEC. The first one was triarylsulfonium hexafluorophosphate (simply referred to as phosphate type or P-type photoinitiator), and the other was triarylsulfonium hexafluoroantimonate (simply referred to as antimonate type or Sb-type photoinitiator). Both were purchased from Sigma Aldrich Co. The densities of the P-type and Sb-type photoinitiators were 1.32 and 1.41 g/mL, respectively, at room temperature. Their chemical structures are described in a previous article.²³

Electron-Beam Curing Process

The electron-beam curing process of DEPC was performed at 2.5 MeV and 8.1 mA at ambient temperature in air with an electron-beam apparatus (ELV-8, EB Technology Co., Korea). The process was carried out by the irradiation of the samples placed on a conveying cart passing through the irradiation spot in the channel with a constant conveying rate. The apparatus for the electron-beam curing process was introduced in the previous article.²³ The as-supplied DEC resin (ca. 15 mL) was placed in aluminum dishes 92 mm in diameter on top of a conveying cart. The conveying speed was 10 m/min throughout the irradiation process. The dose rate was 33.3 kGy/s (10 kGy/scan). The electron-beam absorption doses used were 200, 300, 400, and 600 kGy. We controlled each dose by counting the rotation number of the conveying cart passing through the channel equipped with the electron-beam irradiation facility in the middle of the channel. A dosimetry system by ISO/ASTM 51649 method²⁴ and ISO/ASTM 51650 method²⁵ with a cellulose triacetate film was used. The uncertainty of the electron-beam absorption dose to the samples was less than $\pm 0.5\%$. The total length of the electron-beam emitting window was 1200 mm, and a central zone of 800 mm was used for the irradiation. The thickness of each sample was 2.5–3.0 mm with irradiation at a dose rate ranging from 33.1 to 33.5 kGy/s. The samples were uniformly irradiated through the thickness direction and the surface direction within the uncertainty of the electron-beam absorption dose applied. Table I summarizes the abbreviations designated for each sample irradiated at different doses.

Characterization

To investigate the glass-transition behavior of the DEPC samples irradiated at different electron-beam absorption doses, differential scanning calorimetry (DSC; 200 F3 Maia, Netzsch Co., Germany) was performed from -40 to 150°C with purging nitrogen gas to measure the heat flux change. The heating rate was $10^\circ\text{C}/\text{min}$. The sample weight used for each measurement was about 10 mg.

Thermomechanical analysis (TMA; 2940, TA Instruments) was carried out with purging nitrogen gas to examine the thermal expansion behavior of the DEPC samples irradiated at different absorption doses. A macroexpansion mode was used up to 200°C with a heating rate of $5^\circ\text{C}/\text{min}$ with purging nitrogen gas. Each sample was cut with a low-speed diamond saw (DM-4C, Kye Yang Electronics, Korea). The dimensions of each rectangular-shaped specimen were $5 \times 5 \times 2 \text{ mm}^3$.

Table I. Designations of the Electron-Beam-Cured DEPC Samples Used in This Work

Photoinitiator type	Concentration (wt %)	Electron-beam absorption dose (kGy)
P-type	1	P1 xxx kGy
	2	P2 xxx kGy
	3	P3 xxx kGy
Sb-type	1	Sb1 xxx kGy
	2	Sb2 xxx kGy
	3	Sb3 xxx kGy

^a“xxx” indicates the numerical number of the electron-beam absorption dose applied.

Dynamic mechanical analysis (DMA; Q800, TA Instruments) was carried out to explore the dynamic mechanical thermal properties of the DEPC samples irradiated at different absorption doses. A tension mode was used. The frequency was 1 Hz, the amplitude was 10 μm , and the heating rate was 2°C/min. The measuring temperature range was from -40 to 120°C. Each sample was cut with a low-speed diamond saw (DM-4C, Kye Yang Electronics, Korea). The dimensions of each rectangular-shaped specimen were 35 \times 5 \times 2.5 mm³.

A water absorption test was carried out to examine the extent of water uptake as a function of the immersion time of the DEPC samples irradiated at different absorption doses. Each specimen was placed in a 50-mL vial. The test was performed with an analytical digital scale (model XT220A, Precisa, Switzerland). The weighing precision was ± 0.001 g at ambient temperature. Five specimens were immersed in distilled water to obtain the average value of the percentage water uptake of each sample. Before weighing, each specimen was taken out from the immersion bath, and excess water existing on the outer surfaces of individual specimens was removed with soft tissues by promptly dabbing the surfaces. The test was performed at ambient temperature for 5 weeks. The dimensions of each rectangular-shaped specimen were 10 \times 10 \times 2.5 mm³. The percentage water uptake was obtained from the weight change of each specimen used according to the following equation:^{26,27}

$$\text{Water uptake (\%)} = (W_t - W_i) / W_i \times 100$$

where W_t is the weight of the sample at time t of each test and W_i is the initial weight of the sample before the test.

RESULTS AND DISCUSSION

Electron-Beam-Curing Effect on T_g

In this study, the electron-beam-curing process was performed at 600 kGy or less. The reasons for that were based on our previous study, as follows. According to the variation of the degree of curing as a function of the electron-beam absorption dose for the case of 3 wt % Sb-type photoinitiator in our previous study,²³ the degree of curing of the DEPC at 800 kGy was slightly higher than that at 600 kGy; this indicated that the curing reaction rate became decreased with increasing electron-beam absorption dose higher than 600 kGy. It was also reported that after the electron-beam curing at 800 kGy, the conversion

of cure reaction of the specimens with 2 wt % Sb-type was slightly higher than that with 3 wt % Sb-type. It seemed that the DEPC specimen obtained at 800 kGy was somewhat more brittle than that at 600 kGy. The curing process with the electron beam of low energy was preferable unless the characteristics of the cured DEPC product was meaningfully differentiated. Hence, the electron-beam absorption doses of 600 kGy and less than 600 kGy were used in this study.

Figure 2 shows the variations of T_g of the DEPC with P-type and Sb-type photoinitiators with different concentrations, cured with electron beam at different absorption doses. It was found that T_g of the cured DEPC gradually but slightly increased with increasing electron-beam absorption dose. This could be explained by the fact that the molecular structure of the DEPC became more crosslinked with the dose; this led to restricted molecular motion. Figure 2 also indicates that use of the antimonite-type photoinitiator resulted in a higher T_g than that of the P-type one in the electron-beam curing of DEPC. The higher concentration in the same photoinitiator resulted in a higher T_g of the cured DEPC. That is, P3 600 kGy (-2.9°C) and Sb2 600 kGy (20.9°C) exhibited a higher T_g than P2 600 kGy (-17.4°C) and Sb1 600 kGy (14.1°C) at the corresponding absorption dose, respectively.

Only 2 and 3 wt % P-type photoinitiator and 1 and 2 wt % Sb-type photoinitiator were used in this study on the basis of our previous founding,²³ as described later. According to the appearance of the DEC samples with the P-type and Sb-type photoinitiators cured at various electron-beam absorption doses, unlikely with other cases, the sample with the 1 wt % P-type photoinitiator remained in a liquid state even after the electron-beam irradiation at 800 kGy. Therefore, the sample with 1 wt % P-type was excluded to examine the properties of interest in this study. The concentration of the P-type photoinitiator greater than 3 wt % was also excluded because it was obvious that both the conversion of the curing reaction and the degree of curing were much lower than those of the 1 wt % Sb-type photoinitiator, as reported in the previous study.²³ However, the incorporation of the Sb-type photoinitiator of 3 wt % or higher into the DEC caused some brittleness and darkness of the cured DEPC. In addition, the thermal stability of the cured DEPC samples with 2 and 3 wt % Sb-type photoinitiators, examined by thermogravimetric analysis (TGA) and derivative thermogravimetry (DTG) curves, exhibited almost the same behavior. So, 3 wt % Sb-type samples were excluded for thermal analyses, such as DSC, TMA, and DMA in this study.

Figure 3 represents the variations of T_g as a function of the electron-beam absorption dose according to the photoinitiator used at different concentrations. As shown, the T_g change was most profound with the type of photoinitiator, and it was also significantly influenced by the photoinitiator concentration. However, the electron-beam absorption dose effect on the T_g change was not relatively significant with the exception of P3 200 kGy. The reason for the low T_g value in the case of the P3 200 kGy may be that 200-kGy irradiation was likely low to completely crosslink the DPEC molecule in the presence of P3. In other words, it seemed that 3 wt % P-type photoinitiator

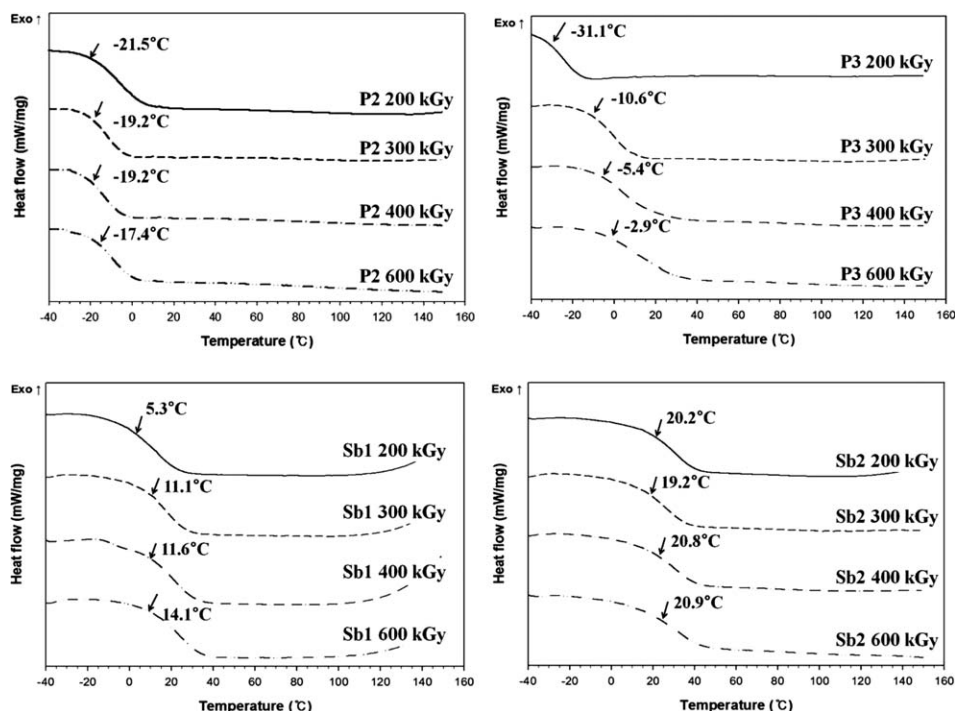


Figure 2. DSC curves of the electron-beam-cured DEPC samples with the Sb-type and P-type photoinitiators. Each T_g value is marked with arrows.

may have been excessive for the electron-beam curing of DEPC at 200 kGy. Epoxy curing by an electron beam could proceed through the ring-opening reaction of epoxide groups by an electron-beam-induced polymerization mechanism via initiation, propagation, and then chain-transfer reactions in the presence of a cationic photoinitiator, as described elsewhere.^{10,13,17} On the basis of the mechanism, the activation of the photoinitiator used may not have proceeded consecutively under the electron-beam irradiation conditions at such a low absorption dose of P3 200 kGy. Hence, the well-developed three-dimensional network structure may not be formed in the case of P3 200 kGy. It was expected that the molecular size of DEPC formed with P3 200 kGy may have been smaller than that of P3 300 kGy and also smaller than that with P2 200 kGy. As a result, the partially cured DEPC was obtained at 200 kGy, even though a photoinitiator concentration of 3 wt % was used. Consequently, the mobility of the partially cured DEPC with less molecular size was less restricted; this resulted in a lower T_g than in the P3 300 kGy and P2 200 kGy cases.

The result reveals that the T_g values (20.2–20.9°C for Sb2 200 kGy to Sb2 600 kGy) of the DEPC electron beam cured with the Sb-type photoinitiator was about 40°C higher than that (–21.5 to –17.4°C for P2 200 kGy to P2 600 kGy) with the P-type photoinitiator at the same concentration. The use of Sb1 exhibited a T_g (14.1°C) about 30°C higher than the use of P2 (–17.4°C) and about 16°C higher than the use of P3 (–2.9°C) at 600 kGy, where complete curing of the DEPC occurred by the electron beam. According to Nishitsuji *et al.*,¹² in the electron-beam curing process of an epoxy resin, the nature of the anion affects the effectiveness of the cationic initiator, and this is inversely related to the nucleophilicity of the anion. The nucleophilicity of SbF_6^- was higher than that of PF_6^- . The

nucleophilicity of the anion of the Sb-type photoinitiator used in our study was higher than that of the P-type photoinitiator. On the basis of the earlier report with epoxy by Park *et al.*,¹³ it may be mentioned that with increasing concentration of the cationic photoinitiator, the probability of the DEPC molecules to encounter and react with the cationic photoinitiator increased, and more cations could transfer to DEC molecules and react with the neighboring cardanol molecules. This led to the curing of DEPC and resulted in the increased T_g . In addition, with increasing electron-beam absorption dose, the probability of the cationic photoinitiator to participate in the curing reaction of DEPC increased; this resulted in an increased degree of curing, as reported in our earlier article.²³ Consequently, we

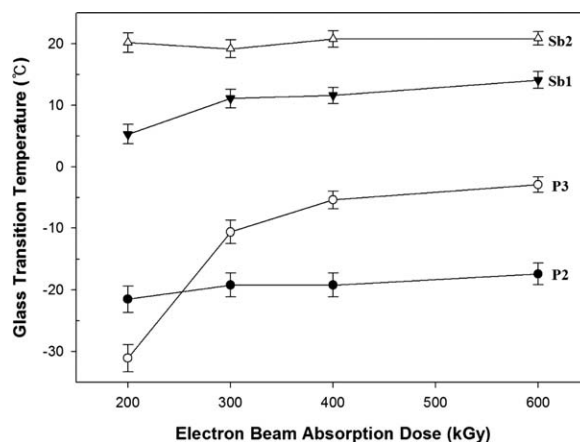


Figure 3. Variations of T_g of the electron-beam-cured DEPC samples with the Sb-type and P-type photoinitiators at different concentrations as a function of the electron-beam absorption dose.

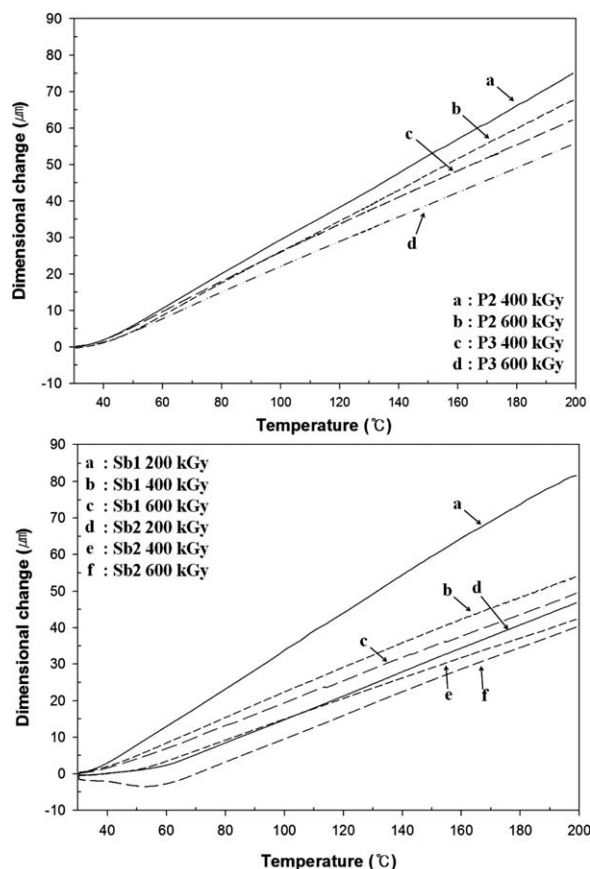


Figure 4. TMA thermograms showing thermodimensional changes in the electron-beam-cured DEPC with the Sb-type and P-type photoinitiators at different concentrations according to the electron-beam absorption dose.

concluded that at low concentrations (Sb1 and Sb2), the Sb-type photoinitiator was more effective for having a T_g of the cured DEPC higher than the P-type photoinitiator. We also noted that Sb2 600 kGy would be optimal for electron-beam curing of the DEPC studied here.

Electron-Beam Curing Effect on the Thermal Expansion Behavior

Figure 4 displays the thermodimensional change of DEPC with different types of photoinitiator and concentrations cured by electron beams at different absorption doses as a function of the temperature. It was obvious that the thermodimensional change reflecting the coefficient of thermal expansion, which could be determined from the slope of each TMA curve, was more or less reduced with the electron-beam absorption dose in the same type and concentration of the photoinitiator used. This was attributed to the formation of an increased network structure in the cured DEPC under the high electron-beam absorption dose; this resulted in the restriction of thermal expansion and the molecular mobility. We also found that the thermodimensional change was lower in P3 than in P2 and lower in Sb2 than in Sb1.

It was convincing that the Sb-type photoinitiator reduced the thermal expansion of the cured DEPC more than the P-type photoinitiator. In addition, Sb2 was more efficient than Sb1 for the

thermodimensional stability of the cured DEPC. The Sb2 600 kGy sample exhibited the lowest dimensional change as a function of the measuring temperature. The coefficient of linear thermal expansion (CLTE) of each sample was determined from the slope of the TMA curve in the temperature range of 50–180°C. The lowest CLTE value ($1.80 \times 10^{-4} \text{C}^{-1}$) of the DEPC sample cured by electron beam was obtained with Sb2 600 kGy. The highest CLTE was $2.56 \times 10^{-4} \text{C}^{-1}$ with P3 200 kGy. The highest value was consistent with the lowest T_g with P3 200 kGy, as previously described. The CLTE value ($1.97 \times 10^{-4} \text{C}^{-1}$) of P3 600 kGy was greater than that of Sb2 600 kGy, and it was rather similar to CLTE of Sb1 600 kGy or Sb2 400 kGy. As a result, we concluded that the Sb-type photoinitiator was more efficient than the phosphate-type one in decreasing the thermal expansion and also increasing the thermodimensional stability of DEPC cured by the electron beam. This result agreed with the variation of T_g , as described previously. The result also revealed that a lower photoinitiator concentration and/or a lower electron-beam absorption dose could be used with the Sb-type photoinitiator for the electron-beam curing of DEPC compared to the case of the P-type photoinitiator. This result also confirms that the electron-beam curing of DEPC with the Sb-type photoinitiator played an effective role in processing the well-cured DEPC product and also in forming the three-dimensional network structure.

Electron-Beam Curing Effect on Dynamic Mechanical Properties

Figure 5 shows the variations of the storage modulus and $\tan \delta$ of the DEPC with different types of photoinitiator and concentrations cured by the electron beam at different absorption doses as a function of the temperature. It was obvious that the storage modulus of the DEPC cured with the Sb-type photoinitiator was considerably higher than that cured with the P-type one. Also, the $\tan \delta$ height of the DEPC with the Sb-type photoinitiator was lower than that with the P-type one. The highest modulus and the lowest $\tan \delta$ were obtained with the DEPC cured with Sb2 600 kGy. On the contrary, the lowest modulus and highest $\tan \delta$ were obtained with P2 200 kGy. The storage modulus was increased in the order Sb2 600 kGy > Sb2 200 kGy > Sb1 600 kGy > Sb1 200 kGy > P2 600 kGy \geq P2 200 kGy. The $\tan \delta$ decreased in the order Sb2 600 kGy < Sb2 200 kGy < Sb1 600 kGy < Sb1 200 kGy < P2 600 kGy < P2 200 kGy. This was explained by the fact that the DEPC molecules cured with the antimonite-type photoinitiator were more crosslinked and stiffer than those with the phosphate-type photoinitiator, as described previously. As shown in Figure 5(A), the storage modulus with Sb2 200 kGy was higher than that with Sb1 600 kGy. This indicated that the concentration of the photoinitiator played a higher contributing role in highly enhancing the storage modulus of the cured DEPC than the electron-beam absorption dose. Of course, the modulus increased with increasing electron-beam absorption dose up to 600 kGy at the same concentration of photoinitiator. We found that an absorption dose higher than 600 kGy was not used because it was rather detrimental to the properties and resulted in some overcured DEPC.

T_g , which could be determined from the peak temperature of the $\tan \delta$ curve, of the DEPC cured with the Sb-type

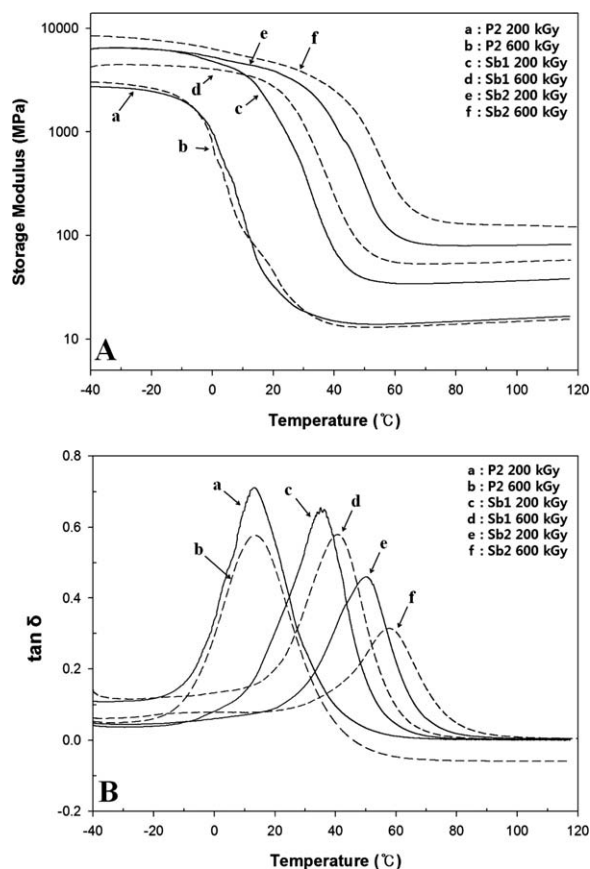


Figure 5. Variations of the storage modulus and $\tan \delta$ curves of the electron-beam-cured DEPC with the Sb-type and P-type photoinitiators at different concentrations as a function of the temperature according to electron-beam radiation.

photoinitiator was higher than that with the P-type one. In the case of the Sb-type, T_g determined by the DMA increased about 22°C from 36 to 58°C with various photoinitiator concentrations and electron-beam absorption dose. In comparison of the T_g values in Figure 2 and Table II, the T_g obtained by the DMA method (Table II) appeared at a higher temperature than that with the DSC method (Figure 2). The difference in T_g between the two thermal analyses occurred because the instrumental mechanisms associated with data acquisition were different. The DMA method is, in general, more sensitive to large-scale molecular motions, even though both methods were based on the thermal events of the polymer molecules.²⁸ The frequency applied in DMA was normally much higher than that analogically interpreted in the DSC measurement; this resulted in a shift of the $\tan \delta$ peak to a higher temperature.²⁹

Table II compares the storage modulus of the cured DEPC examined at three different temperatures. The three temperatures were -40°C, which was far less than T_g of each sample, and 100°C, which was far above T_g . The reason for the choice of these three temperatures follows. The storage modulus at -40°C, which was the initial temperature for the analysis, was at the stage that no significant modulus drop took place for all of the samples used. The storage modulus largely decreased in the glass-transition region, so the modulus change at T_g was

meaningful. A temperature of 100°C was far away from T_g ; this indicated the plateau region of the behavior. Over the all of the measuring temperature range, the storage moduli of the DEPC sample with the Sb-type photoinitiator were greater than those with the P-type one. The greatest storage modulus was obtained from Sb2 600 kGy, as expected. The modulus of 8448 ± 253 MPa at -40°C was considerably decreased to 396 ± 11.9 MPa at T_g and to 126 ± 3.78 MPa at 100°C.

Electron-Beam Curing Effect on the Water Uptake

Figures 6 and 7 display the water-uptake result for the DEPC samples containing the P-type and Sb-type photoinitiators cured at different electron-beam absorption doses, respectively. The testing was carried out for 5 weeks (840 h). With increasing immersion time in distilled water, the percentage water uptake gradually increased up to about 100–170 h; this depended on the photoinitiator type, photoinitiator concentration, and electron-beam absorption dose. After 170 h, the percentage water uptake almost remained constant. Most of the water absorption occurred within 7 to 9 days. The result indicates that the water uptake of the DEPC samples cured with the Sb-type photoinitiator (Figure 7) was less than that with the P-type one (Figure 6). In the case of the P-type photoinitiator, the lowest water uptake (ca. $0.172 \pm 0.006\%$) after 840 h of testing was obtained with P3 600 kGy, whereas the highest value (ca. $0.207 \pm 0.008\%$) was with P2 200 kGy. In the case of the Sb-type photoinitiator, the lowest water uptake (ca. $0.157 \pm 0.006\%$) after 840 h was obtained with Sb3 600 kGy, whereas the highest value (ca. $0.184 \pm 0.007\%$) was with Sb1 200 kGy. With a close inspection (referred to the inserted figures) and a comparison of the effects of the photoinitiator concentration and electron-beam dose, we noticed that the water uptake of the cured DEPC decreased with increasing photoinitiator concentration and electron-beam absorption dose.

The equilibrium time of the water uptake became slightly longer not only with increasing electron-beam absorption dose but also with increasing concentration of the P-type photoinitiator from 2 to 3 wt %. This could be explained by the restriction of the water diffusion in the DEPC specimens and by the fact that the water diffusion was more restricted in the DEPC cured with increasing absorption dose. As a result, the water uptake decreased, and the equilibrium time increased. This phenomenon was more clearly

Table II. Effects of the Electron-Beam Absorption Dose on the T_g and Storage Modulus Values of DEPC Obtained at Three Different Temperatures (-40°C, T_g , and 100°C)

Specimen	T_g (°C)	Storage modulus (MPa)		
		-40°C	T_g	100°C
P2 200 kGy	13.1	2717 ± 82	84 ± 2.5	16 ± 0.5
P2 600 kGy	13.3	3029 ± 91	88 ± 2.6	15 ± 0.5
Sb1 200 kGy	35.6	6296 ± 189	157 ± 4.7	36 ± 1.1
Sb1 600 kGy	40.6	4189 ± 126	224 ± 6.7	56 ± 1.7
Sb2 200 kGy	49.7	6251 ± 188	335 ± 10.1	81 ± 2.4
Sb2 600 kGy	57.6	8448 ± 253	396 ± 11.9	126 ± 3.8

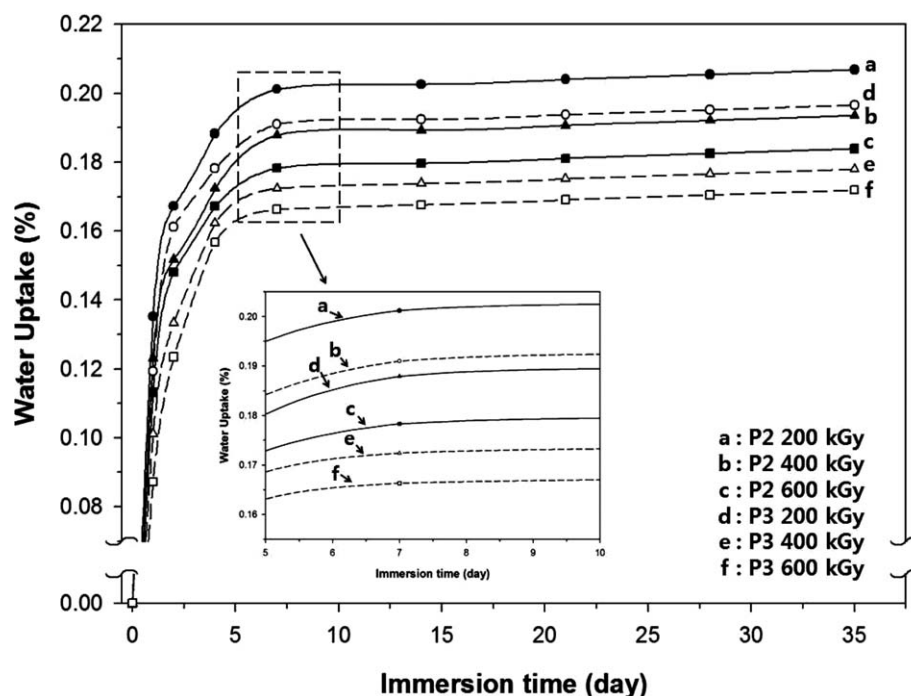


Figure 6. Variations of the water-uptake percentage of the electron-beam-cured DEPC samples with the P-type photoinitiator at different photoinitiator concentrations and electron-beam absorption doses.

found with the DEPC samples containing the Sb-type photoinitiator at different electron-beam absorption doses. With increasing concentration of the Sb-type photoinitiator and the absorption dose, water uptake occurred less, and the equilibration time was shortened.

The reason for the lower water-uptake behavior in the DEPC cured with the Sb-type photoinitiator than that in the P-type photoinitiator was that the Sb-type photoinitiator contributed more to the formation of a crosslinked three-dimensional network structure than the P-type photoinitiator under the

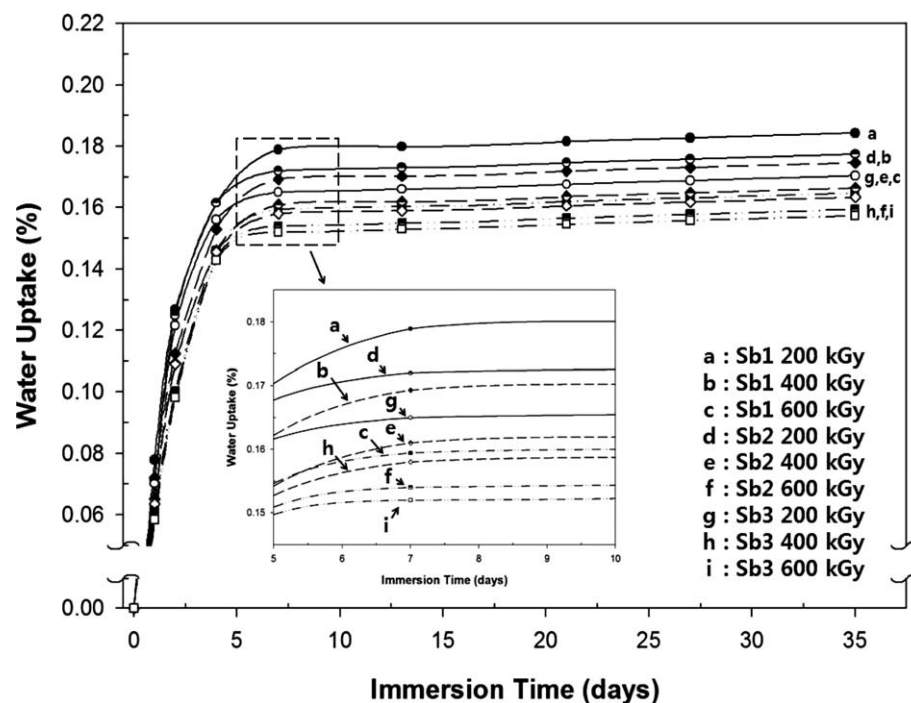


Figure 7. Variations of the water-uptake percentage of the electron-beam-cured DEPC samples with the Sb-type photoinitiator at different photoinitiator concentrations and electron-beam absorption doses.

appropriate electron-beam curing conditions, as described previously in terms of the effect of the photoinitiator type, concentration, and electron-beam absorption dose on T_g . The effect of the photoinitiator type, concentration, and electron-beam absorption dose on the water-uptake result agreed well with the result not only on T_g but also on the thermal expansion behavior and the dynamic mechanical properties of the cured DEPC studied in this work.

CONCLUSIONS

The Sb-type photoinitiator was more desirable for having a T_g of the cured DEPC higher than the phosphate-type photoinitiator and also for lowering the concentration of photoinitiator to be incorporated.

The Sb-type photoinitiator was more efficient than the phosphate-type photoinitiator in decreasing the thermal expansion and also increasing the thermodynamic stability of DEPC cured by the electron beam.

The dynamic mechanical properties of DEPC cured with the Sb-type photoinitiator were considerably higher than those cured with the P-type one. The storage modulus was increased in the order Sb2 600 kGy > Sb2 200 kGy > Sb1 600 kGy > Sb1 200 > P2 600 kGy ≥ P2 200 kGy. The concentration of the photoinitiator played a more contributing role in enhancing the storage modulus of the cured DEPC than the electron-beam absorption dose.

The water uptake of the cured DEPC decreased with increasing photoinitiator concentration and electron-beam absorption dose.

The results on T_g variation, thermal expansion behavior, dynamic mechanical properties, and water uptake of the cured DEPC were quite consistent with each other throughout the study. It implied that the Sb-type photoinitiator was more preferable to the electron-beam curing of DEC, and this led to a lower photoinitiator concentration and electron-beam absorption dose than in the phosphate-type photoinitiator case. It is also recommended that the 2 wt % Sb-type photoinitiator and an electron-beam absorption dose of 600 kGy used in this study may be optimal for the electron-beam curing of DEPC for the formation of a well-developed three-dimensional network structure.

ACKNOWLEDGMENTS

This work was supported by a National Research Foundation of Korea grant funded by the Ministry of Science, ICT, and Future Planning of Korea (contract grant numbers NRF-2012M2B2A4029555 and NRF-2012M2A2A6035747).

REFERENCES

- Ikeda, R.; Tanaka, H.; Uyama, H.; Kobayashi, S. *Macromol. Rapid Commun.* **2002**, *21*, 496.
- Kim, Y. H.; An, E. S.; Park, S. Y.; Song, B. K. *J. Mol. Catal. B* **2007**, *45*, 39.
- Zhou, Q.; Cho, D.; Song, B. K.; Kim, H.-J. *Compos. Interfaces* **2009**, *16*, 781.
- Zhou, Q.; Cho, D.; Park, W. H.; Song, B. K.; Kim, H.-J. *J. Appl. Polym. Sci.* **2011**, *122*, 2774.
- Zhou, Q.; Cho, D.; Song, B. K.; Kim, H.-J. *J. Therm. Anal. Calorim.* **2010**, *99*, 277.
- Govindan, A. *Chem. Eng. World* **1997**, *32*, 79.
- Aziz, S. H.; Ansell, M. P. *Compos. Sci. Technol.* **2004**, *64*, 1231.
- Maffezzoli, A.; Calo, E.; Zurlo, S.; Mele, G.; Tarzia, A.; Stifani, C. *Compos. Sci. Technol.* **2004**, *64*, 839.
- Chen, Z.; Chisholm, B. J.; Webster, D. C.; Zhang, Y.; Patel, S. *Prog. Org. Coat.* **2009**, *65*, 246.
- Nishitsuji, D. A.; Marinucci, G.; Evora, M. C.; Silva, L. G. A. *Nucl. Instrum. Methods Phys. Res. B* **2007**, *265*, 135.
- Sui, G.; Zhang, Z.-G.; Chen, C.-Q.; Zhong, W.-H. *Mater. Chem. Phys.* **2002**, *78*, 349.
- Nishitsuji, D. A.; Marinucci, G.; Evora, M. C.; Silva, L. G. A. *Radiat. Phys. Chem.* **2010**, *79*, 306.
- Park, S. J.; Heo, G. Y.; Lee, J. R.; Suh, D. H. *J. Korean Chem. Soc.* **2003**, *47*, 250.
- Lopata, V. J.; Chung, M.; Janke, C. J.; Havens, S. J. In Proceedings of the 28th International SAMPE Technical Conference, Seattle, WA, Nov 4–7, The Society for the Advancement of Material and Process Engineering, Covina, California, **1996**; p 901.
- Lopata, V. J.; Saunders, C. B.; Singh, A.; Janke, C. J.; Wrenn, G. E.; Havens, S. J. *Radiat. Phys. Chem.* **1999**, *56*, 405.
- Alessi, S.; Dispenza, C.; Fuochi, P. G.; Corda, U.; Lavallo, M.; Spadaro, G. *Radiat. Phys. Chem.* **2007**, *76*, 1308.
- Crivello, J. V.; Walton, T. C.; Malik, R. *Chem. Mater.* **1997**, *9*, 1273.
- Crivello, J. V. *Radiat. Phys. Chem.* **2002**, *63*, 21.
- Park, S. J.; Seo, M. K.; Lee, J. R.; Lee, D. R. *J. Polym. Sci. Part A: Polym. Chem.* **2001**, *39*, 187.
- Crivello, J. V. *J. Polym. Sci. Part A: Polym. Chem.* **1999**, *37*, 4241.
- Endo, T.; Sanda, F.; Toneri, T. *Macromolecules* **2001**, *34*, 1518.
- Takahashi, E.; Sanda, F.; Endo, T. *J. Polym. Sci. Part A: Polym. Chem.* **2002**, *40*, 1037.
- Cheon, J.; Cho, D.; Song, B. K.; Park, J.; Kim, B.; Lee, B. C. *J. Appl. Polym. Sci.* **2015**, *132*, 41599.
- ISO/ASTM 51649: 2005(E). Standard practice for dosimetry in an electron beam facility for radiation processing at energies between 300 keV and 25 MeV. ASTM International, West Conshohocken, PA, **2005**.
- ISO/ASTM 51650: 2005(E). Standard practice for use of a cellulose triacetate dosimetry system, **2005**.
- Dhokal, H. N.; Zhang, Z. Y.; Richardson, M. O. W. *Compos. Sci. Technol.* **2007**, *67*, 1674.
- Alhuthali, A.; Low, I. M.; Dong, C. *Compos. B* **2012**, *43*, 2772.
- Cho, D.; Choi, Y.; Drzal, L. T. *Polymer* **2001**, *41*, 4611.
- Cho, D.; Lee, S.; Yang, G.; Fukushima, H.; Drzal, L. T. *Macromol. Mater. Eng.* **2005**, *290*, 179.